Ecological Modelling 431 (2020) 109159

Contents lists available at ScienceDirect

Ecological Modelling

journal homepage: www.elsevier.com/locate/ecolmodel

Lianas in silico, ecological insights from a model of structural parasitism

Manferdo di Porcia e Brugnera[*,a], Rico Fischer[b], Franziska Taubert[b], Andreas Huth[b,c,d], Hans Verbeeck[a]

[a] CAVElab - Computational and Applied Vegetation Ecology, Ghent University, Ghent, Belgium
[b] Department of Ecological Modelling, Helmholtz Centre for Environmental Research - UFZ, Leipzig, Germany
[c] Institute of Environmental System Research, University of Osnabruck, Osnabruck, Germany
[d] German Centre for Integrative Biodiversity Research iDiv, University of Leipzig, Leipzig, Germany

A B S T R A C T

Tropical forests are a critical component of the Earth system, storing half of the global forest carbon stocks and accounting for a third of terrestrial photosynthesis. Lianas are structural parasites that can substantially reduce the carbon sequestration capacity of these forests. Simulations of this peculiar growth form have only recently started and a single vegetation model included lianas so far. In this work we present a new liana implementation within the individual based model Formind. Initial tests indicate high structural realism both horizontal and vertical. In particular, we benchmarked the model against empirical observations of size distribution, mean liana cluster size and vertical leaf distribution for the Paracou site in French Guiana. Our model predicted a reduction of above-ground biomass between 10% for mature stands to 45% for secondary plots upon inclusion of lianas in the simulations. The reduced biomass was the result of a lower productivity due to a combination of lower tree photosynthesis and high liana respiration. We evaluated structural metrics (LAI, basal area, mean tree-height) and carbon fluxes (GPP, respiration) by comparing simulations with and without lianas. At the equilibrium, liana productivity was 1.9t_C ha^{-1} y^{-1}, or 23% of the total GPP and the forest carbon stocks were between 5% and 11% lower in simulations with lianas. We also highlight the main strengths and limitations of this new approach and propose new field measurements to further the understanding of liana ecology in a modelling framework.

1. Introduction

Lianas are key organisms of tropical forests where they can constitute more than 25 percent of the woody plant species and up to 40 percent of the woody stems (Schnitzer and Bongers, 2011). Lianas are often referred to as structural parasites because although their development starts from the ground, they use existing tree structures to climb up to the top of the canopy. Once in the canopy, lianas deploy large crowns, often blanketing their hosts (Tobin et al., 2012). Lianas compete with trees for both above- (light) and below-ground (water, nutrients) resources (Putz, 1984; Pérez-Salicrup, 2001). Due to lower investment in structural tissues, compared to trees, lianas are left with a greater fraction of carbon to use for reproduction, canopy development, and stem and root elongation (Schnitzer and Bongers, 2002). This shift in allocation to more ephemeral tissues can reduce the carbon residence time in liana abundant forests (Phillips et al., 2005; van der Heijden et al., 2015).

In some regions, like the Neotropics, lianas are increasing in both density and dominance (Phillips et al., 2005). Lianas are particularly well adapted to thrive in forests edges (Campbell et al., 2018), logged areas (Magrach et al., 2016) and disturbed forests in general (Dewalt et al., 2000). Secondary or disturbed forests may provide ideal conditions for liana proliferation by providing an optimal balance of trellises and high light conditions (Madeira et al., 2009). As of 2008, the amount of secondary forest in the Neotropics was estimated to be 2.4 million km^2. Over the next 40 years, this land can potentially accumulate a total above-ground carbon stock of 8.48Pg_C (Chazdon et al., 2016). Lianas have the potential to substantially reduce this carbon sequestration capacity.

Despite lianas being regarded as a key driver of tropical forest change (Lewis et al., 2004), only limited research has addressed their role within a modelling framework. The first process-based model to account for this growth form is the Ecosystem Demography (ED) model (di Porcia e Brugnera et al., 2019). ED is able to capture some features of liana infested forests, e.g. the differential impact across successional stages. However, the underlying structure of ED prevents a realistic representation of a number of liana characteristics. For example, the localized nature of liana effect on their host is harder to represent in a cohort based, spatially implicit model. By simulating single trees, individual based models (IBMs) provide the correct resolution to represent these local processes (Shugart et al., 2018).

In the era of global change, model projections of the land carbon sink are essential to the design of effective mitigation strategies. With this study, we want to test the impact of lianas on the carbon dynamics

* Corresponding author.
E-mail address: manfredo.diporciaebrugnera@ugent.be (M. di Porcia e Brugnera).

https://doi.org/10.1016/j.ecolmodel.2020.109159
Received 14 May 2020; Accepted 29 May 2020

of tropical forest across different successional stages with the IBM Formind (Fischer et al., 2016). Thanks to its structural realism, we expect the new liana plant functional type (PFT) in Formind to capture more accurately than ED the horizontal and vertical distribution of individual lianas and their impact on forest structure. In addition, the individual-based nature of the Formind model allows us to study liana clustering (how many lianas does a tree carry on average?) and whether this property depends on the mechanism through which lianas attach to their host. By upscaling the individual responses to the ecosystem level we also assess the impact of lianas on carbon fluxes such as gross primary productivity (GPP) and net ecosystem exchange (NEE). Output from this type of representation may, if properly validated, be useful to parametrize models with coarser resolution like ED.

2. Methods

2.1. Simulation and data sites

2.1.1. Paracou

All of the simulations presented in this study were conducted at the Paracou site which is located in the coastal part of French Guiana and is classified as a lowland moist primary forest. Records indicate a mean annual precipitation of 3088 mm, with a well-marked dry season from mid-August to mid-November. The floristic composition is highly diverse with high standing biomass (Guitet et al., 2014). We used a simplified meteorological forcing (Hiltner et al., 2018) that assumed the length of the daily photosynthetic active period to be 12h (Köhler et al., 2003) and the mean annual irradiance above the canopy to be 694$\mu mol_{photons}\ m^{-2}\ s^{-1}$ (Huth and Ditzer, 2000).

For this study we used inventories that were conducted in 10 plots of undisturbed forest. These 70 m × 70 m plots were established in 2004 in the Paracou flux-tower footprint. In 2015 all lianas with $DBH \geq$ 2cm were censused using the standard protocol (Gerwing et al., 2006), for a total of 839 lianas over a 4.9ha area. During the same field campaign, the intrinsic quantum yield and the light-saturated photosynthesis were measured for 10 liana individuals (Pausenberger, 2016) with a CIRAS-3 instrument. In a successive field campaign in 2016, terrestrial laser scans (TLS) were performed to estimate the forest vertical structure and the plant area index (PAI) (Pieters, 2017).

2.1.2. Other sites

To derive liana growth parameters, we used diameter inventories that were collected for a total of 4623 lianas at the Gigante Peninsula site in Panama (Schnitzer and van der Heijden, 2019). The inventories were carried out in 2011 and 2014 and we calculated the yearly DBH increments by averaging over this 3-year period. For size distributions we compared simulations results with data from Paracou and literature data of two additional sites. The first one is Point Calimere Wildlife Sanctuary (PCWS), a 2 hectares, tropical dry evergreen forest site in south-east India (Pandi and Parthasarathy, 2017). The second one is YasunÃ National Park (YNP), a 0.4 hectares, tropical moist forest site in Ecuador (Nabe-Nielsen, 2001).

2.2. Liana functional type in formind

Formind is an individual-based, spatially explicit, process-based model designed for simulating species-rich vegetation communities (Fischer et al., 2016). Each hectare is partitioned with a 20 m × 20 m grid for a total of 25 plots per hectare. Competition for light and space takes place at the plot level but tree positions are not resolved within the plot. The demographic processes considered are recruitment, growth and mortality.

To model the light climate within the forest canopy, vertical canopy layers are discretized with 0.5 m strata. Temporarily, the model is discretized with yearly time steps. For more details about the model structure we refer to the original model description (Fischer et al., 2016).

For this work we developed a new liana plant functional type. The challenge was to include processes in the Formind model to capture the scandent physiology of the liana growth form. In the next paragraphs we describe in detail the representation of the liana PFT and the parameters that we used.

2.2.1. Recruitment

Like trees, new lianas in Formind are recruited with a seed rain that happens whenever the available light is higher than a predefined threshold. As such, the recruitment process is governed by two parameters: available light (as a fraction of total incoming radiation) and number of seeds for ingrowth. Each year, if the light conditions are met, a plot will receive a number of new individuals N_{new} equal to

$$N_{new} = \lfloor \frac{N_{seeds}}{N_{plots}} \rfloor \quad (1)$$

where N_{seeds} is the seed ingrowth parameter and N_{plots} is the number of plots per hectare. If the number of ingrowing seeds is not a multiple of the number of plots, the remaining seeds will be distributed randomly to the plots. As very little data is available to parametrize this process, we assumed liana seed ingrowth to be equal to the maximum used for trees (high seed production). We also assumed the minimum light threshold for seed ingrowth to be equal to the average value used for tree PFTs. The parameters are shown in Table 1. We assumed that upon establishment all lianas and trees have an initial stem diameter of 1cm.

2.2.2. Growth

In the model, lianas undergo three main stages of developmental growth: (1) self-supporting, (2) climbing and (3) in the canopy

Table 1
Model parametrization. The numbers for the 8 tree PFTs are expressed as a range (or as a single number when all trees have the same parameter). For tree PFT-specific values we refer to Hiltner et al. (2018). Liana values are presented with the corresponding literature reference or with a derivation description.

Parameter	Unit	Trees	Liana	Reference
LAI (individual)	$m^2\ m^{-2}$	2	1.2	Putz (1983)
Seed ingrowth (N_{seeds})	$ha^{-1}\ y^{-1}$	2 - 27	27	Tree maximum
Percent of full light for seed establishment	%	1 - 20	6	Tree average
Stochastic baseline mortality rate *	y^{-1}	0.03 - 0.05	0.0149	Putz (1990)
Form factor (f)	-	0.425 - 0.97	1	See Methods (Biomass)
Maximum leaf photosynthesis	$\mu mol_{CO_2}\ m^{-2}\ s^{-1}$	1.12 - 27	8.1	Pausenberger (2016)
Intrinsic quantum yield	$\mu mol_{CO_2}\ \mu mol^{-1}_{photons}$	0.035 - 0.086	0.031	Pausenberger (2016)
Wood density (ρ)	$g\ cm^{-3}$	0.55 - 0.83	0.40	Putz (1990)
Maximum height	m	16.5 - 40.4	40.4	Tree maximum
Stem factor (S)	% of total AGB in main stem	0.7	0.78	See Methods (Biomass)

* Trees have an additional mortality rate that depends on their DBH and on their yearly DBH increment (Fischer et al., 2016). Lianas have an additional, process based, mortality that is described in Section 2.2.3

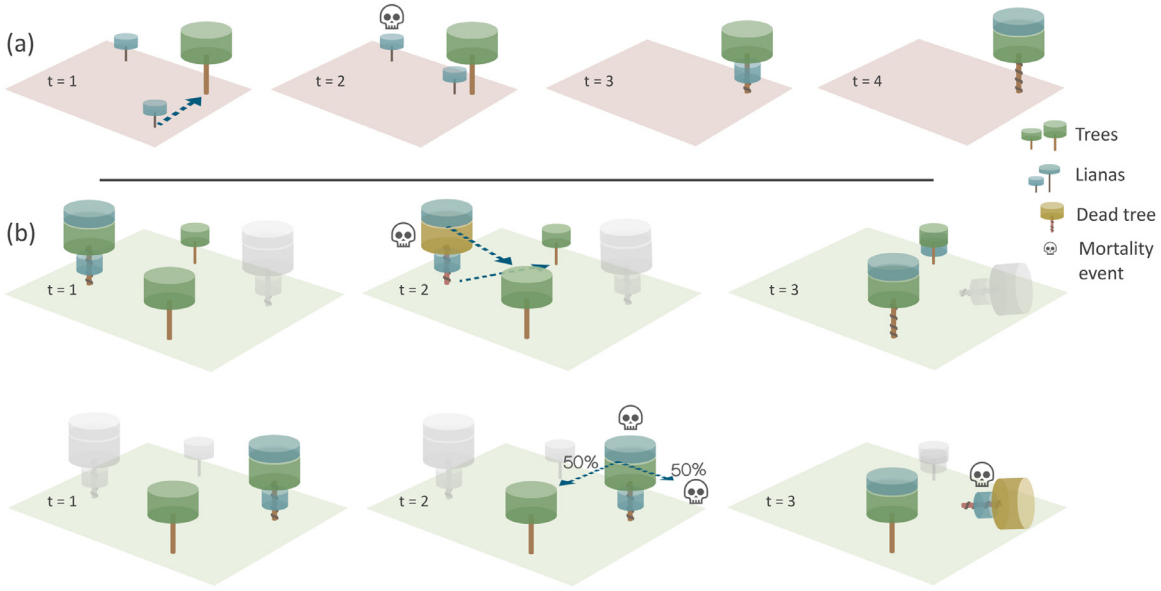

Fig. 1. Schematic illustration of developmental growth stages (a) and mortality (b) of lianas in Formind. Lianas start their development as self-supporting. They then stochastically find a host and start to climb up until reaching the top of the canopy. Like trees, lianas have a stochastic baseline mortality (see t = 2 of (a)). In addition to the baseline mortality, depending on their development stage and on their host death mode lianas either move to a different host or die. If the hosting tree dies without falling, lianas move to a different host regardless of whether they are climbing or already in the canopy top (upper strip of (b)). If their host falls, climbing lianas die while lianas that were on top of the canopy have a 50% chance of surviving and moving to a different host of similar size (lower strip of (b)).

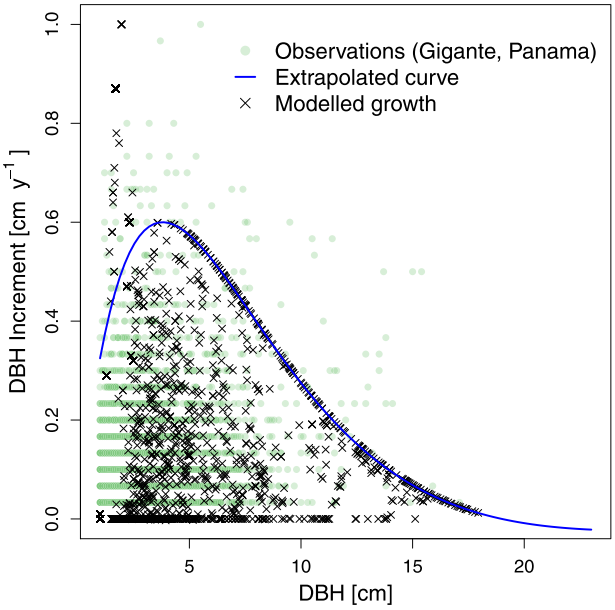

Fig. 2. Relation between DBH and yearly DBH increase for lianas. Observations for the Gigante site are shown with green points. The blue curve is derived from the observations (Fischer, 2010). Black crosses are simulated growth values. For small DBH values, modelled growth can occasionally lie above the characteristic curve if lianas are self-supporting (tree-like growth curve). A large number of lianas have zero DBH increments, an analysis of this specific result is provided in Appendix B. (For interpretation of the references to colour in this figure legend, the reader is referred to the web version of this article.)

(Fig. 1a). When in the self-supporting stage lianas are assigned a "virtual" tree PFT, whereby they inherit the growth curve of a randomly chosen tree PFT. As a result, the diameter growth of self-supporting lianas is similar to the one used for trees until they find a host (Fig. 2).

Once a liana finds a suitable host, it enters stage 2 where net primary productivity (NPP) is used exclusively for vertical elongation. Stem diameter and crown area are kept constant until the liana reaches the host canopy.

Once in the canopy top (stage 3), liana height is constrained to its host height and stem growth is derived from a growth curve. The growth curve is a prescribed function that assigns a maximum annual diameter increase for each diameter. The curve was obtained by fitting the Gigante observations of diameter increase with a characteristic function as described in Fischer (2010). The function is shown as a blue line in Fig. 2.

Crown ratio (crown length divided by tree height) is assumed to be the same for lianas and trees until stage 3. Once in the top of the canopy, we assumed lianas to deploy all of their leaves in the highest stratum that the tree crown is occupying (Avalos et al., 2007). Canopy area for lianas depends on their developmental stage and is described in detail in Appendix B.

2.2.3. Mortality

Mortality in Formind is a stochastic process that every annual time step kills each individual with a certain probability. Trees can die of multiple causes including background mortality, diameter dependent mortality, diameter increment dependent mortality, crowding and damage by a falling dead tree, or by external disturbance events like logging, fires or landslides (Fischer et al., 2016).

Like trees, lianas have a fixed background mortality rate (Table 1). Once climbing, the liana mortality is complemented with a new, process-based mortality that depends on the mortality of their host. This additional mortality depends on both, the fate of the dying host and on the growth stage of the liana. Fig. 1b provides a schematic representation of these processes which were developed based on mechanical considerations. If the hosting tree dies without falling it is assumed that lianas can find a new host. If the hosting tree falls, the liana dies if it has not yet reached the top of the canopy, and either dies or moves to a new host if it is already in the top of the canopy (with a 50% chance). This last condition was constructed assuming that lianas in the top of the canopy may be attached to multiple hosts and hence be able to withstand the fall of their main host.

2.2.4. Biomass

While trees in the Formind model have a one to one correspondence

between diameter and biomass, a certain degree of variability exists for lianas due to the non-bijective nature of the height-diameter relation (liana height is host-dependent rather than DBH-dependent). In Formind, given a plant height H [m], its biomass AGB [t_C] is calculated as

$$AGB = \frac{\pi}{4}\cdot(DBH)^2\cdot H\cdot\rho\cdot f\cdot\frac{1}{S} \quad (2)$$

Where DBH [m] is the stem diameter, ρ [$t_C\ m^{-3}$] is the wood density, f is the form factor and S is the stem factor. The form factor accounts for the tapering of the stem. While for trees the form factor is a function of DBH, for lianas we assumed $f = 1$ (perfect cylinder). The stem factor S is the proportion between the total tree AGB and the biomass of the main stem, thus providing a correction for branches and leaves. Given that for lianas $f = 1$, S^{-1} becomes the ratio between the actual biomass and the biomass of a cylinder of equivalent diameter and height (thus including shape corrections such as for helical stem structure).

Assuming an accurate tree vertical structure (H of Eq. (2)), we calculated the optimal stem factor to match the observed liana AGB allometry (Schnitzer et al., 2006). We used a bisection algorithm to estimate the S value that minimized the root mean square deviation between our simulations (letting S vary) and the published allometry, obtaining a value of $S = 0.78$ (Fig. 3).

2.2.5. Liana-host interactions

The selection of the liana host has two possible pathways. In the first one, which we will refer to as method 1, possible hosts are all trees in the plot. In the second one, which we will refer to as method 2, we also include other lianas as possible hosts. For both methods, the only requirement we impose is that the potential host height should be higher than the liana height. Once a host is selected, the attachment is a stochastic process with a probability P(DBH)[y^{-1}]. The probability was constructed based on the observed probability of finding lianas in the canopy as a function of their DBH (Kurzel et al., 2006). The probability is given by

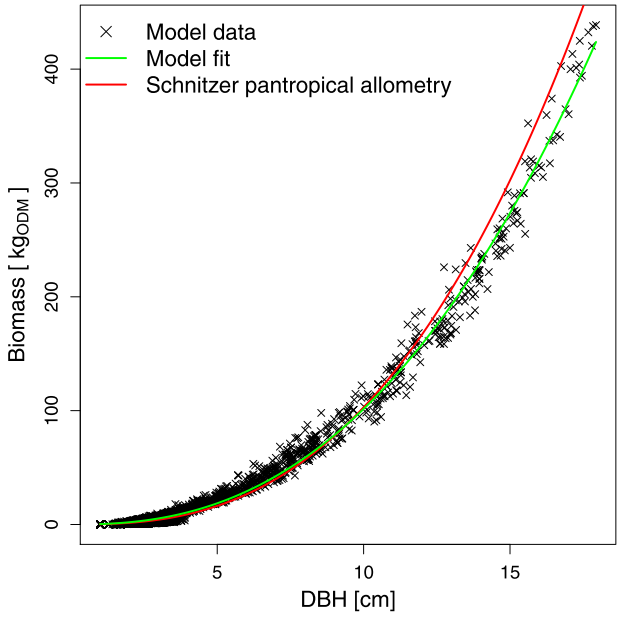

Fig. 3. Liana simulated biomass (black points) in kilograms of organic dry mass ($1kg_{ODM} = 0.44kg_C$, (Scherer, 1995)). Model data fit is shown in green and liana published allometry (Schnitzer et al., 2006) is shown in red. (For interpretation of the references to colour in this figure legend, the reader is referred to the web version of this article.)

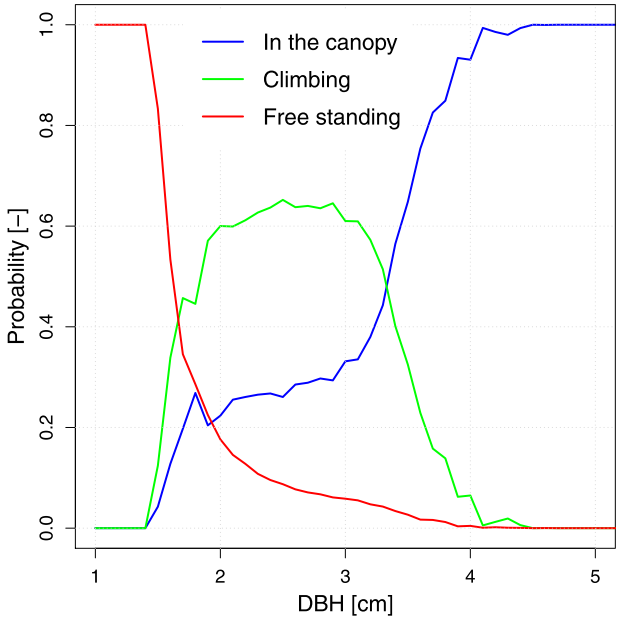

Fig. 4. Simulated probability of lianas to be found in the three distinct stages of development. The probabilities are derived from model simulations at the equilibrium (year 400 to 500).

$$P(DBH) = \begin{cases} 0 & DBH < 1.5\text{cm} \\ 1 & DBH > 4\text{cm} \\ \frac{f(DBH)-f(1.5)}{f(4)-f(1.5)} & elsewhere \end{cases} \quad (3)$$

where $f(x) = \frac{1}{1+e^{-k(x-\mu)}}$ is the logistic function with $k = 2$ and $\mu = 2.5$. The parameter k controls the steepness of the curve so that for large k the function becomes linear. μ is the midpoint of the sigmoidal curve, so that $f(\mu) = 0.5$. This type of probability ensures a realistic fraction of lianas in the different stages of growth as shown in Fig. 4. We tested different distributions, e.g. linear interpolation, and the results were similar.

Experimental evidence suggests that a single liana is able to colonize multiple trees (Ichihashi and Tateno, 2011; Putz, 1984). From an ecological viewpoint this could have multiple benefits for lianas: mechanically it would reduce the risk of falling (Ichihashi and Tateno, 2011) and the increased vertical and horizontal growth (Putz, 1984) due to liana's specific physiology could lead to higher photosynthesis and deployment of leaves in optimal conditions. Although our model allows multiple lianas to colonize a single tree, only one host is allowed for each liana. To compensate for this limitation, we allowed lianas to change their host when light conditions are sub-optimal (Roeder et al., 2015). More specifically, if a liana has reached its host canopy but still receives less that 50% of the total incoming radiation, we assign a 10% y^{-1} probability of switching to a new host. The new host is selected randomly within all trees taller than the current host that satisfy the criterion $h_T - h_L < 2$m where h_L is the liana height and h_T is the new host height. As we have seen, host change can also take place if the liana host dies, as described in the mortality section. In this case we only require that $|h_L - h_T| < 2m$ to prevent large discontinuities in height.

2.2.6. Liana impact on trees

Lianas are known to affect the architecture of their hosts. Studies have shown that significant liana loads alter tree allometry by decreasing slenderness (Dias et al., 2017) and that lianas replace tree leaves on a one-to-one biomass basis (Ogawa et al., 1965). However, the specific impact of lianas on tree leaves remains uncertain and a recent study failed to find correlation between liana canopy area and understory measurements (Cox et al., 2019).

In our model, leaf area index (LAI) and crown ratio (CR) of the hosting tree are affected by the proportion of liana and tree leaves. Given the original LAI and the original crown ratio CR of the host tree, its new parameters LAI' and CR' are calculated as

$$LAI' = f \cdot LAI \quad (4)$$

$$CR' = f \cdot CR \quad (5)$$

where

$$f = \frac{AC_T + \frac{AC_L}{2}}{AC_T + AC_L} \quad (6)$$

is a reduction factor and AC_T and AC_L are the total crown area of the tree and of the lianas on it, respectively. A detailed analysis of the consequences of this penalization scheme is presented in Appendix B. This penalization is the only modification that was made to trees in the Formind model for this study.

2.3. Parametrization

To parametrize the liana PFT we used a combination of published and non-published data. If the required parameter was not available in literature we resorted to realistic assumptions. For recruitment we derived the parameters from other PFTs by using the maximum number of seed ingrowth used for trees and averaging the light threshold for establishment. For the maximum height we assumed lianas to be able to climb all tree PFTs in the simulation, thus assigning a maximum height equal to the maximum tree height. Parameters and the corresponding references are presented in Table 1; the range of values for the tree PFTs are also given for comparison.

2.4. Simulation details

The simulated 16 hectares were initialized from bare ground and were continued for 500 years to reach an equilibrium state. The runs with and without lianas were performed with the same conditions but turning on and off the liana PFT. Liana densities were measured by sampling all attached lianas with $DBH \geq 2$ cm. In addition to liana density, the realism of the simulated distribution of lianas within the hosting trees (i.e. number of lianas per host tree) was tested by comparing simulations for Paracou with observations at YNP and PCWS. The total number of modelled leaf strata was 81, equal to the ceiling of maximum tree height (40.4 m) divided by the height layer width (0.5 m). Vertical leaf profiles were derived by aggregating leaf area contribution of each plant for every height strata. To assess the impact of lianas on the different tree size classes, trees were categorized based on three levels of infestation: free, low and high liana load. When the liana crown area was less than half that of its host, the tree was classified as having low liana load, otherwise the tree was classified with high liana load. Gas exchanges were calculated at the plant level and aggregated for every individual to obtain forest level GPP and autotrophic respiration. Heterotrophic respiration was calculated adding respiration from dead wood biomass and the fast and slow-cycling components of soil respiration. NEE was calculated as GPP minus the autotrophic and heterotrophic respiration. For the complete description of the carbon cycle in Formind we refer to Fischer et al. (2016).

2.5. Statistics

Correlations between liana density and mean liana age and tree basal area were calculated using the Pearson's correlation test. To study liana clustering, trees with one liana were tested to find whether they had a higher probability of having more than one liana (Nabe-Nielsen, 2001; Putz, 1984). Expected Poisson distributions were generated with the parameter λ equal to the simulated data (average number of lianas per tree). Expected and simulated distributions were compared using a χ^2 goodness-of-fit test. Trees hosting 3 or more lianas were aggregated to avoid expected values smaller than one. Fits for liana counts were performed by linearizing the data and using a least squares fit. All statistical analyses were performed in R version 3.5.1 (R Core Team, 2018). Unless differently specified, model results are presented as mean ± standard deviation of the 16 hectares.

3. Results

3.1. Size and spatial distribution of lianas

Simulations gave an overall liana density of 333 ± 170individuals ha^{-1} while observed data showed a lower density of 171stems ha^{-1}. In terms of liana basal area, the model predicted a value of 0.46 ± 0.14cm^2 m^{-2} compared to an observed value of 0.42cm^2 m^{-2}. In the model, large lianas ($DBH \geq 10$cm) accounted for 41 ± 13% of the total liana basal area, similar to the empirical observation of 40% (around 30% in a large-scale study in Peru, Phillips et al. (2005)). Liana density across different hectares was negatively correlated with mean liana age (Pearson's correlation; $r = -0.58$, $p = 0.017$) and tree basal area (Pearson's correlation; $r = -0.47$, $p = 0.06$) indicating that lianas decrease in abundance with forest succession. The model was able to qualitatively reproduce the trend in size distribution observed at Paracou (Fig. 5). Compared to the observed size distribution, the model slightly overestimated the fraction of small lianas ($DBH < 5$cm) and underestimated the fraction of larger lianas. The large variability among the different hectares can be traced back to different light environments (due to their disturbance history) and to stochastic effects.

Despite Paracou, YNP and PCWS being different types of forest, the simulated pattern of liana cluster size had a similar exponential decay (YNP: $y = 784e^{-0.97x}$; PCWS: $y = 604e^{-0.81x}$; this study: $y = 449e^{-0.86x}$, Fig. 6). The similarity of the modelled decay constant to the observed ones indicates that the model may be able to capture the tree-liana and liana-liana competition for space and light.

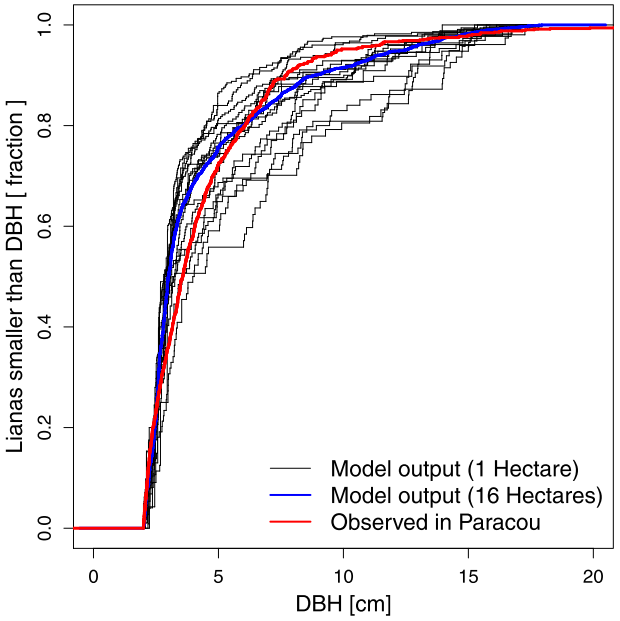

Fig. 5. Normalized cumulative distribution of lianas as a function of their DBH. Black curves correspond to the 16 different hectares of the simulation. The blue curve is the total area average of the simulation while the red curve is the observed distribution at Paracou. In Paracou 5 lianas had $DBH > 20$cm which explains why the red curve saturation is not yet reached at 20cm (which is the maximum DBH for simulated lianas in Formind). (For interpretation of the references to colour in this figure legend, the reader is referred to the web version of this article.)

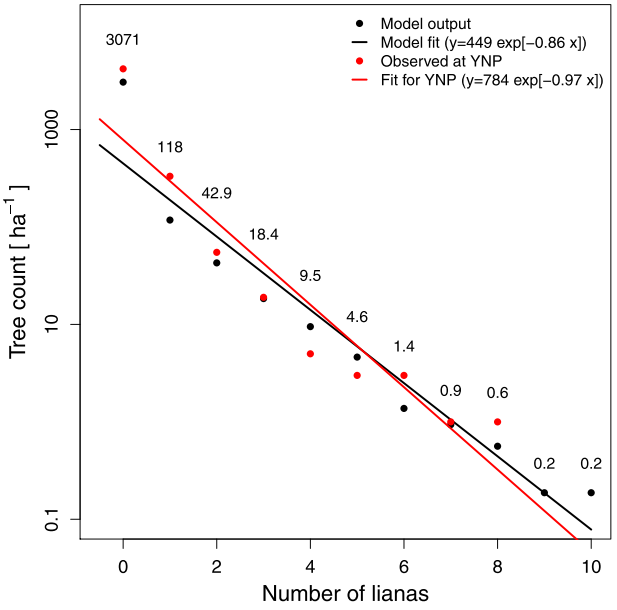

Fig. 6. Number of lianas per tree for Paracou (black) and Yasuní (YNP, red). Numbers are the simulated liana counts. Both datasets were fitted with an exponential decay function. YNP data reproduced with permission from Nabe-Nielsen (2001). (For interpretation of the references to colour in this figure legend, the reader is referred to the web version of this article.)

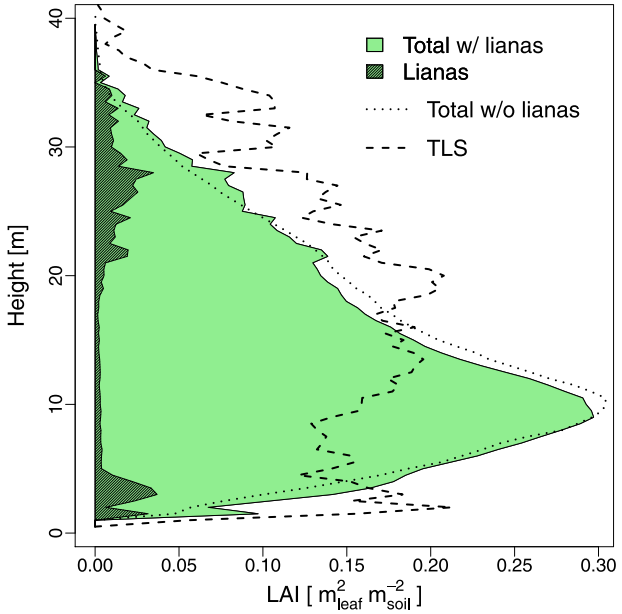

Fig. 7. Modelled vertical distribution of leaf area index (green) with liana component (grey shade). The dashed line is the vertical distribution of plant area index observed with TLS and the dotted line is the vertical distribution of the model without lianas. (For interpretation of the references to colour in this figure legend, the reader is referred to the web version of this article.)

We also tested the impact of the two different attachment mechanisms: with method 1, the simulated liana count per tree was perfectly random upon attachment; by contrast, if lianas could use other lianas to climb the canopy (method 2), the liana count was skewed towards larger clusters as trees with more lianas became stronger attractors. To test whether the model kept memory of the initial distribution (sample of all lianas of age 1), we extracted the simulated liana count per host at the equilibrium. The number of trees with two or more lianas was larger than would be expected by chance with both method 1 ($\chi^2 = 59563$, $df = 3$, $p < 0.0001$; Table A.1) and method 2 ($\chi^2 = 67121$, $df = 3$, $p < 0.0001$; Table A.2), suggesting that lianas tend to aggregate.

The loss of memory of the initial distribution was consistent with the implementation of a routine that allows lianas to change their host. The mean liana cluster size was 1.59 and 1.57 for method 1 and 2 respectively. The similarity of these numbers suggests that upon reaching equilibrium, liana clusters adjust to an optimal size to avoid conspecific competition. Liana clumping was time dependent; after year 50 of the simulation, mean cluster size slightly increased over time for both attachment mechanisms (Fig. A.1).

3.2. Leaf profiles

Total simulated LAI of the Paracou site was 4.93 ± 0.1 m^2 m^{-2} compared to a TLS-observed PAI of 5.17 m^2 m^{-2}. As it includes contributions from trunks and branches, PAI is expected to be slightly higher than LAI. Comparison between simulations and TLS showed that the model overestimated total LAI at low heights and underestimated it above 15 m, Fig. 7. Liana leaves tended to occupy the higher strata of the canopy with 62% of the leaves found above 20 m when the forest is at the equilibrium. Although the overall liana LAI was 6.9 ± 2.4% of the total, it grew to 17.3 ± 6.4% for the 20 m–30 m stratum and to 38.3 ± 22.0% for the 30 m–40 m stratum. The significant proportion of liana leaves simulated below 5 m was due to the high liana seedling density, as a result of our reproduction parametrization. We point out that while the simulations considered 16ha of forest, the TLS scans were taken at 9 plots close to the flux tower and may not represent an accurate forest average. Introduction of lianas in the simulations did not significantly affect the total amount and distribution of leaves (Fig. 7, dotted curve).

3.3. Simulations with and without lianas

3.3.1. Biomass and forest structure

We compared simulations with and without lianas to assess their impact on forest structure and carbon stocks. One of the most dramatic effects of lianas was the reduced basal area across the entire forest succession. After 50 years, basal area of the forest with lianas was about half that of the forest without lianas (16.9 ± 0.8 m^2 ha^{-1} vs 30.6 ± 1.5 m^2 ha^{-1} respectively). This difference was due to a lower plant density (10521 vs 11374 plants for the 16 hectares, respectively) and to a lower average tree diameter (16.2 ± 9.2cm vs 18.9 ± 13.3cm, respectively). The quadratic dependency of basal area upon DBH amplified this difference (Fig. 8a). After the forest equilibrated, mean basal area was still lower in the presence of lianas (28.4 ± 2.2 m^2 ha^{-1} vs 32.1 ± 1.7 m^2 ha^{-1}).

Mean adult tree height was proportionally less impacted by lianas than basal area (Fig. 8a) because, unlike basal area, tree height is a concave function of DBH. After 50 years, mean adult tree height was 16.6 ± 0.1 m for the simulation with lianas and 17.6 ± 0.1 m for the simulation without lianas; at the equilibrium, there was no significant difference for this metric. After year 60 of the simulation, total LAI was generally higher for the simulation with lianas, however the difference was always less than 5%. At the equilibrium, LAI for the simulation with lianas was about 2% higher than the non-liana simulation, with lianas accounting for circa 7% of the total leaf area.

Results from simulations showed a strong impact of lianas on stand level above ground biomass. The reduction of AGB was more pronounced in the early stage of succession when lianas were more abundant, Fig. 8(b, c). The maximum reduction in biomass was 43% when the forest was 45 years old. After 100 years, the reduction in AGB was 13% and fluctuated between 5 and 11% after reaching the equilibrium. The simulated value of AGB at year 500 was 185 ± 15t$_C$ ha^{-1} while empirical observations estimated AGB at 186 ± 7t$_C$ ha^{-1} (Rutishauser et al., 2010). At the individual level, we analysed the

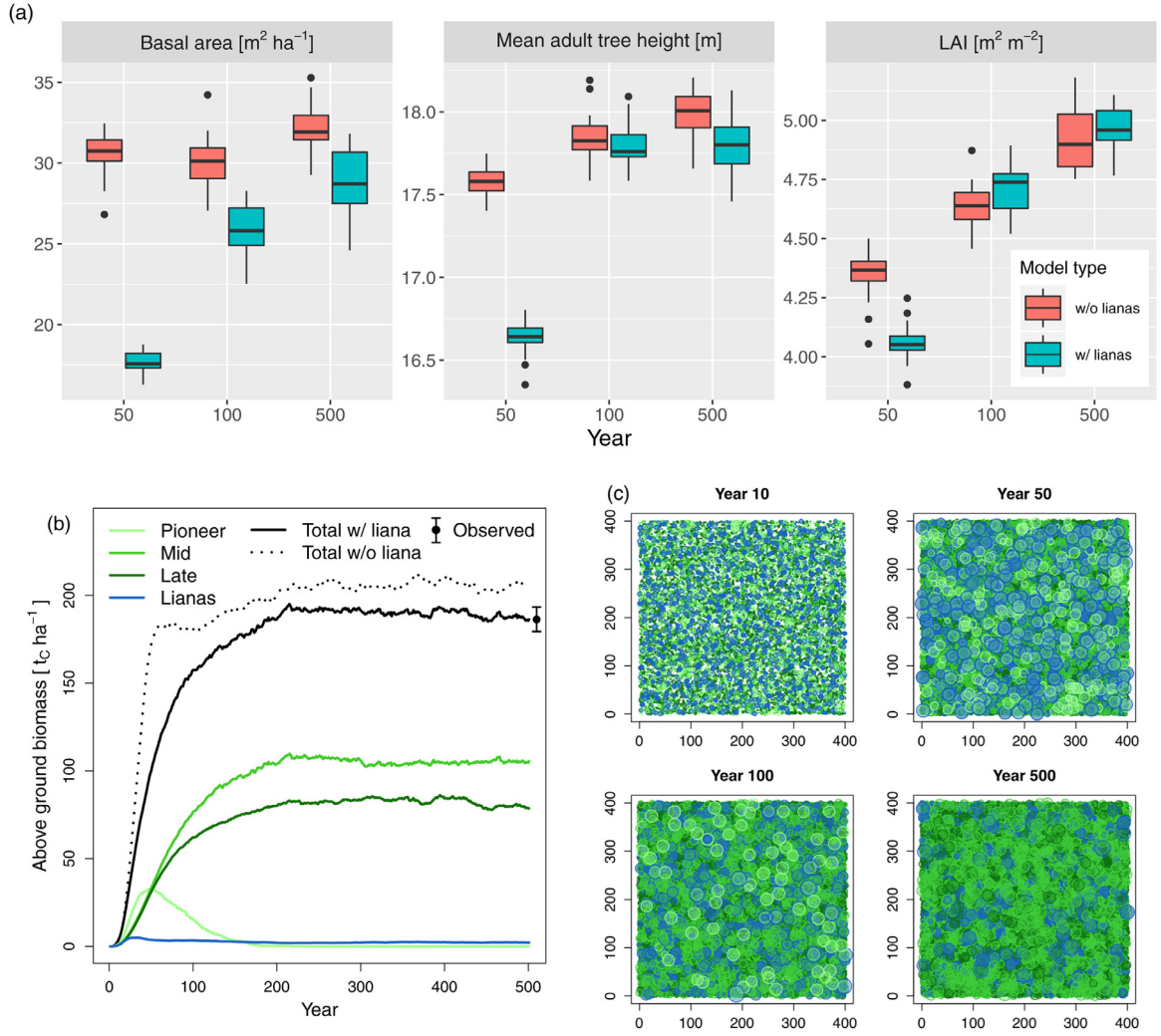

Fig. 8. 16 one-hectare variability of structural metrics for simulation years 50, 100 and 500 with and without lianas. Box plots show the median as the solid black line and the first and third quartiles as the limits of the box. Whiskers extend up to 1.5 times the interquartile range (a). Biomass time series for a simulation from bare ground (b) and above-canopy view of simulated crown distribution (c). In panel (b) solid lines refer to the run with the liana PFT while the dashed line refers to the simulation without lianas. Observed AGB value was calculated for trees with *DBH* ≥ 10cm. PFT colour scheme for (b) and (c) is the same.

Table 2
Yearly biomass increments for trees with no, low or high liana load for different size classes in kg of organic dry mass (mean for years 100 to 500). The high standard deviation of the data is due to the highly variable irradiance that trees are exposed to, even within the same DBH class.

Yearly biomass increment [kg_{ODM}]	10cm-30cm	30cm-50cm	50cm-80cm	> **80cm**
No Liana	8.4 ± 5.9	34.7 ± 8.8	54.9 ± 11.4	79.9 ± 42.0
Low liana load	7.6 ± 5.2	28.6 ± 7.3	51.1 ± 11.0	76.4 ± 38.6
High liana load	6.8 ± 6.1	26.0 ± 6.7	40.9 ± 7.6	48.6 ± 25.5

mean biomass increments (averaged over the simulation from year 100 to year 500) for three different classes of liana infestation and for four different tree size classes. As expected, yearly biomass increments were lower with increasing liana load (Table 2) for all size classes. For the taller canopy trees (*DBH* > 80cm), mean biomass increment with high liana load was only 64% of the one for trees without lianas.

The biomass impact per PFT showed a correlation with successional stage and with tree maximum height. For example, when a pioneer PFT peaked in abundance, its total biomass was up to 70% less upon inclusion of lianas (PFT 4, Fig. A.2). PFTs that reach lower maximum heights were proportionally less impacted by lianas (see PFTs 1, 2 and 3 of Fig. A.2). These results are consistent with the ability for lianas to move up the canopy and with the absence of any host-PFT-specific process.

3.3.2. Carbon fluxes

Carbon fluxes were sensitive to the introduction of lianas in the simulations. Liana maximum photosynthetic rate was assumed to be higher than climax species but lower than pioneers (Table 1). As a result, GPP in the simulation with lianas was lower (maximum reduction of 46% at year 50) than in the simulation without lianas when pioneers are abundant, that is until year 100–120. For the same reason, GPP for the simulation with lianas was up to 20% higher at the equilibrium when the PFT composition shifted towards shade tolerance. Maximum liana GPP was 5.5t_C ha^{-1} y^{-1} at year 24 (38% of the total GPP). The average liana contribution to GPP for the years 400 to 500 was 1.9t_C ha^{-1} y^{-1} (23% of the total, Fig. 9a).

Autotrophic respiration was also impacted by the introduction of lianas. The trend in the first 100 years of succession was similar to the one observed for GPP with lianas reducing total respiration by up to 51%. The simulated liana contribution to biomass respiration was high throughout the succession and, at the equilibrium, accounted for 54% of the total 3.44t_C ha^{-1} y^{-1} respired by vegetation. After year 250, biomass respiration with lianas was almost twice that of the simulation

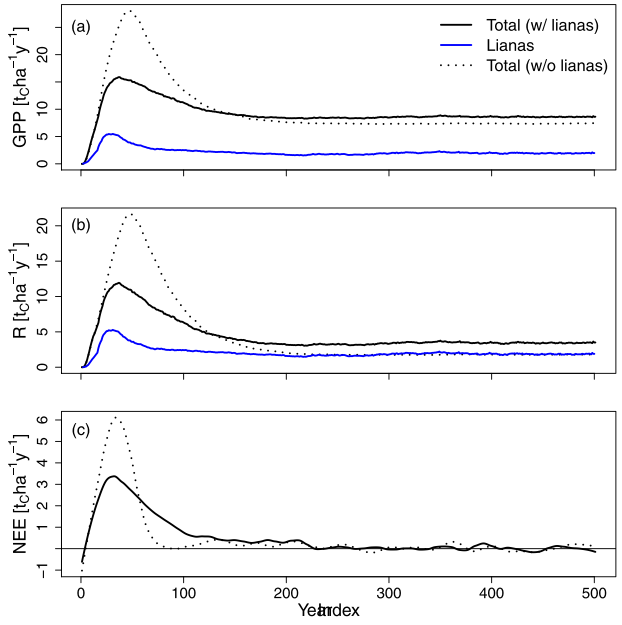

Fig. 9. Gross primary productivity (a), autotrophic respiration (b) and net ecosystem exchange (c) for the simulations with (solid line) and without (dashed line) lianas. Liana contribution to GPP and respiration is shown in blue. (For interpretation of the references to colour in this figure legend, the reader is referred to the web version of this article.)

without lianas (Fig. 9b). These trends can be understood in light of the very low diameter growth rate for lianas which resulted in a large fraction of GPP respired back to the atmosphere.

NEE converged to zero more slowly when lianas were included in the model. This result was consistent with the observed ability for lianas to slow down the ecosystem succession (Tymen et al., 2016). Despite being positive for about 250 years, lianas reduced the maximum yearly carbon uptake by about 50%, Fig. 9c. By integrating NEE over the entire simulation, we found that the total carbon sink for the liana-free forest was 8% higher (261.4t_C ha^{-1} vs 240.1$t_C$ha^{-1}). There was a compensation effect of heterotrophic respiration which, unlike biomass respiration, was always lower when lianas were included (Fig. A.3). The lower value of heterotrophic respiration was the consequence of a forest with lower AGB but similar AGB mortality rate. At the equilibrium, carbon residence time (AGB / NPP) was ~ 36 years regardless of the inclusion of the liana PFT.

4. Discussion

4.1. Model structure

Our liana model introduces a custom representation for the climber growth form that is able to distinguish between three phases of ontogeny (Fig. 4). The probabilistic transition between the different growth phases was constructed based on logical assumptions. In fact, the model is likely overestimating the fraction of lianas in the climbing stage and smaller lianas should have a higher probability of being in the canopy compared to the current probability in the model (for example compare Fig. 4 with Fig. 1 of Kurzel et al. (2006)). Albeit only qualitative, this multi-phase structure constitutes a significant improvement over the representation of lianas in ED, where the climbing phase was not explicitly represented (di Porcia e Brugnera et al., 2019). Future modelling efforts seeking to simulate lianas throughout their development will benefit from field data that discriminates lianas as self-supporting, climbing or in the canopy. Equally important for a realistic model will be a statistic / mechanistic understanding of the transition from one stage to the next.

One of the key features of the Formind model is the calculation of growth and respiration from observed diameter increments. In woody vines, annual diameter growth has been shown to be substantially lower than trees (on average 1.4 mm y^{-1} vs 6 mm y^{-1} for the BCI site, Putz (1990)) as a result of a markedly different allocation pattern. In our liana representation, the low values of diameter growth prevented proper liana establishment. As a correction, we simulate growth of self-supporting lianas as if they were trees. This use of a virtual tree PFT for lianas could be extended to canopy lianas, especially when a tree trait distribution is similar to a liana trait distribution, e.g. for leaf mass area (Wyka et al., 2013).

In addition to growth, most other mechanisms describing lianas were built with some degree of speculation. For example, host dynamic (the ability for lianas to change their host) relies on the assumption that lianas will move across the canopy seeking better light conditions. The probability (which we assumed to be 10%. y^{-1}) to find a new host when light conditions are sub-optimal needs additional enquiry, even though experimental measurements will be challenging to obtain. In the model, host dynamic was also connected to tree mortality; the fate of lianas on dying trees is still unclear and needs to be addressed with more observations if we are to construct a realistic mortality process.

Finally, although some studies have tried to understand liana impact on trees at an individual level (Dias et al., 2017; Ogawa et al., 1965; van der Heijden et al., 2010), a more thorough analysis of shading and mechanical stress is needed to improve our tree penalization scheme.

4.2. Model findings

Size distribution Size distributions result from the interplay of many different processes and, being one of the most common field measurement, are an important model benchmark. Our liana implementation proved successful in capturing the qualitative trend in size distribution (Fig. 1). To confirm that the underlying processes and their parametrization are realistic, these results will need additional testing, in sites with different external conditions. Total liana density was about twice the observed one, however it should be noted that, compared to other sites, liana density in Paracou is particularly low (DeWalt et al., 2015). The bulk of this overestimation was for lianas with *DBH* < 5cm which may be explained by the high value of the recruitment rate parameter and to the fact that observations in the old-growth Paracou plots may not have had tree fall disturbances recently.

Clustering and horizontal distribution Our model predicted a clumped individual distribution with an average cluster size of around 1.6 lianas. Since this result was independent of the attachment mechanism, the clustering is likely to be driven by host change and light and space competition. From a modelling point of view, host change is a necessary feature to ensure that lianas stay in the higher part of the canopy. Although this assumption of lianas seeking better light condition is reasonable, its mechanistic representation and the host change probability should be evaluated against new observations. If host change makes liana more likely to colonize the same trees, light and space competition bind this process by making large clusters prone to conspecific competition. As we have seen the exponential decay constant of liana cluster size is similar between modelled and observed data. This suggests that the implementation of light competition and crowding mortality that was developed for trees can be generalized to lianas.

Leaf profiles In lowland tropical forests, light is one of the most limiting resources (Kitajima et al., 2005). Vertical leaf profiles are an important metric to understand how light is extinguished while reaching the understory. Recent technological developments, such as laser scanning (Krishna Moorthy et al., 2018), have allowed to measure these quantities with greater precision, however, these instruments cannot parse the different components of the leaf profile (i.e. species, growth form). In our simulations, lianas deployed the majority of their leaves in the higher part of the canopy. This result, while consistent

with lianas expected behaviour, is a significant improvement over the previous liana model where liana leaves were concentrated only at low heights. The introduction of lianas did not significantly alter the forest LAI as a whole, suggesting that lianas substitute tree leaves in similar spatial locations. The small LAI bulge at low heights was due to the large number of saplings and to the contribution of plots where a tree fall event occurred. Although observations confirm that lianas abound in correspondence of canopy openings (Schnitzer et al., 2000), the parameters for seed dispersion may be overestimated. In this sense the addition of more liana PFTs with a broad trait dispersion could be a solution to ensure establishment under the highly variable light conditions of the 500 years simulation.

Biomass Liana impact on AGB was strong both at an individual level and at the landscape level. At the individual level, tree penalization resulted in smaller biomass increments when the host had a high liana load (due to a reduced LAI). To test our penalization scheme, field measurement of trees with and without lianas would be needed. As it is unlikely to find trees with similar characteristics but varying liana loads, such measurements can only be of statistical nature. At the plot level these types of comparison have already started (van der Heijden et al., 2019) and may be used in the future to better parametrize liana burden on trees.

Carbon fluxes Overall, most of the reduction in biomass could be accounted for by the very high rate of respiration in lianas (discussed in Appendix B). As Formind does not explicitly represent leaves and fine roots, much of the GPP that is not used for growth is thus respired. In reality, part of this GPP is likely to be used for production of tissues with fast turnover rates like leaves or fine roots (Zhu and Cao, 2010). Since the model does not explicitly represent these allocation processes, the carbon is directly re-emitted through respiration instead of going through litter decomposition; in other words, the model is overestimating autotrophic respiration and underestimating heterotrophic respiration. Given that the carbon residence time of leaves and fine roots is short, this simplification may have little consequences in terms of carbon fluxes. An inclusion of more realistic mortality impact of lianas to their host (such as by considering mechanical stress) may result in shorter carbon residence time and thus an even lower forest carbon sink potential.

4.3. Additional considerations

In the current stage, the model clumps the entire diversity of climbers into one liana PFT. This is a strong limitation as climbers appear in about half (Putz et al., 1991) of vascular plant families and their trait spectra are known to be dispersed (Wyka et al., 2013). The development of additional liana PFTs, for example a shade-tolerant liana (Nabe-Nielsen, 2004) may also reduce the strong impact of lianas on respiration. Furthermore, many aspects of the climber growth form have not been considered, e.g. below-ground competition or host specificity. As many studies have linked liana abundance to hydrology, for example finding correlations between liana abundance and mean annual precipitation or precipitation seasonality (Dewalt et al., 2000), a greater model complexity needs to be incorporated to make general predictions of ecological value.

From a computational point of view, the addition of lianas often introduces a second order cost because of the interaction with trees. For example, when calculating the LAI penalization due to lianas, the model needs to check each tree for all of its lianas. An additional computational burden is due to the use of open arrays; these could be simplified by assuming a maximum number of lianas per tree. In terms of model structure, both Formind and ED are now able to simulate trees, grasses and lianas. Both models make use of keywords to create parallel computational regions for each growth form. In the case of Formind or other models written in object-oriented languages, we advise for a greater use of polymorphism and inheritance to make the code more compact and abstract. For example, most allometric equations now require an explicit check of the growth form whenever they are used. The use of a parent plant class could help to hide these specific implementations from where these methods are called. Finally, for researchers interested in implementing lianas in different models, we advise to start with two liana PFTs. Although the complexity from one PFT is normally more than enough to start, the use of a second, dummy PFT can help to create more robust and general code from the start.

5. Conclusions

Liana modelling is still in its infancy and this work should lay the ground for additional investigations, including with the use of new modelling frameworks. With Formind we were able to capture many aspects of a liana infested forest. In particular we concentrated on correctly reproducing demography and spatial distributions. In the current stage, the model could already be tested on real scenarios, for example quantifying liana impact on carbon stocks in disturbed or logged forests, or making forecasts for the future of liana removal plots. To expand the applicability of the present model - for example to produce regional estimates - we advise to first test the model under the extremely variable climate, soil and topographical conditions under which lianas are found.

Author contributions

MDP lead the model development and data analysis with contributions from FT and RF. All authors contributed to discussions and revised the final version of the manuscript.

Declaration of Competing Interest

The authors declare that they have no known competing financial interests or personal relationships that could have appeared to influence the work reported in this paper.

The authors declare the following financial interests/personal relationships which may be considered as potential competing interests:

Acknowledgments

This study was funded by the European Research Council Starting Grant 637643 (TREECLIMBERS) and the special research fund of Ghent University (BOF project 01N00816). Special thanks to M. Piantoni for her help with the graphics of Fig. 1.

Supplementary material

Supplementary material associated with this article can be found, in the online version, at 10.1016/j.ecolmodel.2020.109159.

References

Avalos, G., Mulkey, S.S., Kitajima, K., Wright, S.J., 2007. Colonization strategies of two liana species in a tropical dry forest canopy. Biotropica 39 (3), 393–399. https://doi.org/10.1111/j.1744-7429.2007.00265.x.

di Porcia e Brugnera, M., Meunier, F., Longo, M., Krishna Moorthy, S.M., De Deurwaerder, H., Schnitzer, S.A., Bonal, D., Faybishenko, B., Verbeeck, H., 2019. Modeling the impact of liana infestation on the demography and carbon cycle of tropical forests. Glob. Chang Biol. 25 (11), 3767–3780. https://doi.org/10.1111/gcb.14769.

Campbell, M.J., Edwards, W., Magrach, A., Alamgir, M., Porolak, G., Mohandass, D., Laurance, W.F., 2018. Edge disturbance drives liana abundance increase and alteration of liana-host tree interactions in tropical forest fragments. Ecol. Evol. 8 (8), 4237–4251. https://doi.org/10.1002/ece3.3959.

Chazdon, R.L., Broadbent, E.N., Rozendaal, D.M.A., Bongers, F., Zambrano, A.M.A., Aide, T.M., Balvanera, P., Becknell, J.M., Boukili, V., Brancalion, P.H.S., Craven, D., Almeida-Cortez, J.S., Cabral, G.A.L., de Jong, B., Denslow, J.S., Dent, D.H., DeWalt, S.J., Dupuy, J.M., Durán, S.M., Espírito-Santo, M.M., Fandino, M.C., César, R.G., Hall, J.S., Hernández-Stefanoni, J.L., Jakovac, C.C., Junqueira, A.B., Kennard, D., Letcher, S.G., Lohbeck, M., Martínez-Ramos, M., Massoca, P., Meave, J.A., Mesquita, R., Mora, F., Muñoz, R., Muscarella, R., Nunes, Y.R.F., Ochoa-Gaona, S., Orihuela-Belmonte, E., Peña-Claros, M., Pérez-García, E.A., Piotto, D., Powers, J.S., Rodríguez-Velazquez, J.,

Romero-Pérez, I.E., Ruíz, J., Saldarriaga, J.G., Sanchez-Azofeifa, A., Schwartz, N.B., Steininger, M.K., Swenson, N.G., Uriarte, M., van Breugel, M., van der Wal, H., Veloso, M.D.M., Vester, H., Vieira, I.C.G., Bentos, T.V., Williamson, G.B., Poorter, L., 2016. Carbon sequestration potential of second-growth forest regeneration in the latin american tropics. Sci. Adv. 2 (5). https://doi.org/10.1126/sciadv.1501639.

Cox, C.J., Edwards, W., Campbell, M.J., Laurance, W.F., Laurance, S.G.W., 2019. Liana cover in the canopies of rainforest trees is not predicted by local ground-based measures. Austral Ecol. 44 (5), 759–767. https://doi.org/10.1111/aec.12746.

DeWalt, S.J., Schnitzer, S.A., Alves, L.F., Bongers, F., Burnham, R.J., Cai, Z., Carson, W.P., Chave, J., Chuyong, G.B., Costa, F.R.C., Ewango, C.E.N., Gallagher, R.V., Gerwing, J.J., Amezcua, E.G., Hart, T., Ibarra-Manríquez, G., Ickes, K., Kenfack, D., Letcher, S.G., Macía, M.J., Makana, J.-R., Malizia, A., Martínez-Ramos, M., Mascaro, J., Muthumperumal, C., Muthuramkumar, S., Nogueira, A., Parren, M.P.E., Parthasarathy, N., Pérez-Salicrup, D.R., Putz, F.E., Romero-Saltos, H.G., Sridhar Reddy, M., Sainge, M.N., Thomas, D., Melis, J.v., 2015. Biogeographical Patterns of Liana Abundance and Diversity. 27. John Wiley & Sons, Ltd, Chichester, UK, pp. 131–146.

Dewalt, S.J., Schnitzer, S.A., Denslow, J.S., 2000. Density and diversity of lianas along a chronosequence in a central panamanian lowland forest. J. Trop. Ecol. 16 (1), 1–19. https://doi.org/10.1017/s0266467400001231.

Dias, A.S., dos Santos, K., dos Santos, F.A.M., Martins, F.R., 2017. How liana loads alter tree allometry in tropical forests. Plant Ecol. 218 (2), 119–125. https://doi.org/10.1007/s11258-016-0671-0.

Fischer, R., 2010. Modellierung des Wachstums von Regenwäldern. Untersuchung der Auswirkungen von Trockenstress und Holznutzung auf den tropischen Regenwald am Beispiel des RNI Betampona (Madagaskar). Phd.

Fischer, R., Bohn, F., de Paula, M.D., Dislich, C., Groeneveld, J., Gutiérrez, A.G., Kazmierczak, M., Knapp, N., Lehmann, S., Paulick, S., Pütz, S., Rödig, E., Taubert, F., Köhler, P., Huth, A., 2016. Lessons learned from applying a forest gap model to understand ecosystem and carbon dynamics of complex tropical forests. Ecological Modelling 326, 124–133. https://doi.org/10.1016/j.ecolmodel.2015.11.018. Next generation ecological modelling, concepts, and theory: structural realism, emergence, and predictions

Gerwing, J., Schnitzer, S., Burnham, R., Bongers, F., Chave, J., DeWalt, S., Ewango, C., Foster, R., Kenfack, D., Martinez-Ramos, M., Parren, M., Parthasarathy, N., Pérez-Salicrup, D., Putz, F., Thomas, D., 2006. A standard protocol for liana censuses. Biotropica 38, 256–261. https://doi.org/10.1111/j.1744-7429.2006.00134.x.

Guitet, S., Sabatier, D., Brunaux, O., Hérault, B., Aubry-Kientz, M., Molino, J.-F., Baraloto, C., 2014. Estimating tropical tree diversity indices from forestry surveys: a method to integrate taxonomic uncertainty. For. Ecol. Manage. 328, 270–281. https://doi.org/10.1016/j.foreco.2014.05.045.

Hiltner, U., Huth, A., Bruning, A., Hérault, B., Fischer, R., 2018. Simulation of succession in a neotropical forest: high selective logging intensities prolong the recovery times of ecosystem functions. For. Ecol. Manage. 430, 517–525. https://doi.org/10.1016/j.foreco.2018.08.042.

Huth, A., Ditzer, T., 2000. Simulation of the growth of a lowland dipterocarp rain forest with formix3. Ecol. Modell. 134 (1), 1–25. https://doi.org/10.1016/S0304-3800(00)00328-8.

Ichihashi, R., Tateno, M., 2011. Strategies to balance between light acquisition and the risk of falls of four temperate liana species: to overtop host canopies or not? J. Ecol. 99 (4), 1071–1080. https://doi.org/10.1111/j.1365-2745.2011.01808.x.

Kitajima, K., Mulkey, S.S., Wright, S.J., 2005. Variation in crown light utilization characteristics among tropical canopy trees. Ann. Bot. 95 (3), 535–547. https://doi.org/10.1093/aob/mci051.

Krishna Moorthy, S., Moorthy, S.K., Calders, K., di Porcia e Brugnera, M., Schnitzer, S., Verbeeck, H., 2018. Terrestrial laser scanning to detect liana impact on forest structure. Remote Sens. 10 (6), 810. https://doi.org/10.3390/rs10060810.

Kurzel, B.P., Schnitzer, S.A., Carson, W.P., 2006. Predicting liana crown location from stem diameter in three panamanian lowland forests1. Biotropica 38 (2), 262–266. https://doi.org/10.1111/j.1744-7429.2006.00135.x.

Köhler, P., Chave, J., Riera, B., Huth, A., 2003. Simulating the long-term response of tropical wet forests to fragmentation. Ecosystems 6, 0114–0128. https://doi.org/10.1007/s10021-002-0121-9.

Lewis, S.L., Malhi, Y., Phillips, O.L., 2004. Fingerprinting the impacts of global change on tropical forests. Philos. Trans. R. Soc. Lond. B 359 (1443), 437–462. https://doi.org/10.1098/rstb.2003.1432.

Madeira, B.G., Espírito-Santo, M.M., Neto, S.D., Nunes, Y.R.F., Arturo Sánchez Azofeifa, G., Wilson Fernandes, G., Quesada, M., 2009. Changes in Tree and Liana Communities Along a Successional Gradient in a Tropical Dry Forest in South-Eastern Brazil. Springer Netherlands, Dordrecht, pp. 291–304.

Magrach, A., Senior, R.A., Rogers, A., Nurdin, D., Benedick, S., Laurance, W.F., Santamaria, L., Edwards, D.P., 2016. Selective logging in tropical forests decreases the robustness of liana–tree interaction networks to the loss of host tree species. Proc. R. Soc. B 283 (1826), 20153008. https://doi.org/10.1098/rspb.2015.3008.

Nabe-Nielsen, J., 2001. Diversity and distribution of lianas in a neotropical rain forest, Yasuní National Park, Ecuador. J. Trop. Ecol. 17 (1), 1–19.

Nabe-Nielsen, J., 2004. Demography of machaerium cuspidatum, a shade-tolerant neotropical liana. J. Trop. Ecol. 20 (5), 505—516. https://doi.org/10.1017/S0266467404001609.

Ogawa, H., Yoda, K., Ogino, K., Kira, T., 1965. Comparative ecological studies of three main types of forest vegetation in Thailand, 2: plant biomass. Nat. Life Southeast Asia 4, 49–80.

Pandi, V., Parthasarathy, N., 2017. Patterns of tree-liana interactions: distribution and host preference of lianas in a tropical dry evergreen forest in India. Trop Ecol 58, 591–603.

Pausenberger, N., 2016. Photosynthetic Characteristics of Lianas Versus Trees in Tropical Rainforest in French Guiana. Master's thesis.

Phillips, O.L., Vásquez Martínez, R., Monteagudo Mendoza, A., Baker, T.R., Núñez Vargas, P., 2005. Large lianas as hyperdynamic elements of the tropical forest canopy. Ecology 86 (5), 1250–1258.

Pieters, S., 2017. The Influence of Lianas on Tropical Forest Structure Using Terrestrial Laser Scanning. Master's thesis.

Putz, F.E., 1983. Liana biomass and leaf area of a "tierra firme" forest in the rio negro basin, venezuela. Biotropica 15 (3), 185. https://doi.org/10.2307/2387827.

Putz, F.E., 1984. The natural history of lianas on Barro Colorado Island, Panama. Ecology 65 (6), 1713–1724. https://doi.org/10.2307/1937767.

Putz, F.E., 1990. Liana stem diameter growth and mortality rates on Barro Colorado Island, Panama. Biotropica 22 (1), 103–105.

Putz, F.E., Mooney, H.A., et al., 1991. The Biology of Vines. Cambridge University Press.

Pérez-Salicrup, D.R., 2001. Effect of liana cutting on tree regeneration in a liana forest in Amazonia Bolivia. Ecology 82 (2), 389–396. https://doi.org/10.1890/0012-9658(2001)082[0389:EOLCOT]2.0.CO;2.

R Core Team, 2018. R: A Language and Environment for Statistical Computing. R Foundation for Statistical Computing. Vienna, Austria.

Roeder, M., Slik, J.F., Harrison, R.D., Paudel, E., Tomlinson, K.W., 2015. Proximity to the host is an important characteristic for selection of the first support in lianas. J. Veg. Sci. 26 (6), 1054–1060. https://doi.org/10.1111/jvs.12316.

Rutishauser, E., Wagner, F., Herault, B., Nicolini, E.-A., Blanc, L., 2010. Contrasting above-ground biomass balance in a neotropical rain forest. J. Veg. Sci. https://doi.org/10.1111/j.1654-1103.2010.01175.x.

Scherer, H.W., 1995. Larcher, W. (Hrsg.): Ökophysiologie der Pflanzen. Ulmer Verlag, stuttgart 1994; 360 S., DM 78,- (ISBN 3-8252-8074-8). Zeitschrift für Pflanzenernhrung und Bodenkunde 158 (2). https://doi.org/10.1002/jpln.19951580214. 207–207

Schnitzer, S.A., Bongers, F., 2002. The ecology of lianas and their role in forests. Trends Ecol. Evol. 17 (5), 223–230. https://doi.org/10.1016/S0169-5347(02)02491-6.

Schnitzer, S.A., Bongers, F., 2011. Increasing liana abundance and biomass in tropical forests: emerging patterns and putative mechanisms. Ecol. Lett. 14 (4), 397–406. https://doi.org/10.1111/j.1461-0248.2011.01590.x.

Schnitzer, S.A., Dalling, J.W., Carson, W.P., 2000. The impact of lianas on tree regeneration in tropical forest canopy gaps: evidence for an alternative pathway of gap-phase regeneration. J. Ecol. 88 (4), 655–666. https://doi.org/10.1046/j.1365-2745.2000.00489.x.

Schnitzer, S.A., DeWalt, S.J., Chave, J., 2006. Censusing and measuring lianas: a quantitative comparison of the common methods1. Biotropica 38 (5), 581–591. https://doi.org/10.1111/j.1744-7429.2006.00187.x.

Schnitzer, S.A., van der Heijden, G.M.F., 2019. Lianas have a seasonal growth advantage over co-occurring trees. Ecology 100 (5), e02655. https://doi.org/10.1002/ecy.2655.

Shugart, H., Wang, B., Fischer, R., Ma, J., Fang, J., Yan, X., Huth, A., Armstrong, A., 2018. Gap models and their individual-based relatives in the assessment of the consequences of global change. Environ. Res. Lett. 13. https://doi.org/10.1088/1748-9326/aaaacc.

Tobin, M.F., Wright, A.J., Mangan, S.A., Schnitzer, S.A., 2012. Lianas have a greater competitive effect than trees of similar biomass on tropical canopy trees. Ecosphere 3 (2), art20. https://doi.org/10.1890/ES11-00322.1.

Tymen, B., Réjou-Méchain, M., Dalling, J.W., Fauset, S., Feldpausch, T.R., Norden, N., Phillips, O.L., Turner, B.L., Viers, J., Chave, J., 2016. Evidence for arrested succession in a liana-infested Amazonian forest. J. Ecol. 104 (1), 149–159. https://doi.org/10.1111/1365-2745.12504.

van der Heijden, G.M., Feldpausch, T.R., de la Fuente Herrero, A., van der Velden, N.K., Phillips, O.L., 2010. Calibrating the liana crown occupancy index in Amazonian forests. For. Ecol. Manage. 260 (4), 549–555. https://doi.org/10.1016/j.foreco.2010.05.011.

van der Heijden, G.M., Powers, J.S., Schnitzer, S.A., 2015. Lianas reduce carbon accumulation and storage in tropical forests. Proc. Natl. Acad. Sci. 112 (43), 13267–13271. https://doi.org/10.1073/pnas.1504869112.

van der Heijden, G.M., Powers, J.S., Schnitzer, S.A., 2019. Effect of lianas on forest-level tree carbon accumulation does not differ between seasons: results from a liana removal experiment in Panama. J. Ecol. 107 (4), 1890–1900. https://doi.org/10.1111/1365-2745.13155.

Wyka, T.P., Oleksyn, J., Karolewski, P., Schnitzer, S.A., 2013. Phenotypic correlates of the lianescent growth form: a review. Ann. Bot. 112 (9), 1667–1681. https://doi.org/10.1093/aob/mct236.

Zhu, S.-D., Cao, K.-F., 2010. Contrasting cost-benefit strategy between lianas and trees in a tropical seasonal rain forest in southwestern China. Oecologia 163, 591–599. https://doi.org/10.1007/s00442-010-1579-3.